# A study on small-world brain functional networks altered by postherpetic neuralgia

Yue Zhang[1], Jing Liu[2], Jing Wang[1], Minyi Du[3], Wenxue Fang[3], Dongxin Wang[3], Xiaopin Hu[4], Xuexiang Jiang[2], Jing Fang[1], Xiaoying Wang[2], and Jue Zhang[1]

[1]*Peking University, Beijing, Beijing, China,* [2]*Department of Radiology, Peking University First Hospital, Beijing, Beijing, China,* [3]*Department of Anesthesiology, Peking University First Hospital, Beijing, Beijing, China,* [4]*Department of Biomedical Engineering, Georgia Institute of Technology / Emory University, Atlanta, Georgia, United States*

**Introduction:** Living with chronic pain impacts one's life quality negatively. peripheral neuropathic pain (PNP), originated from injury or dysfunction of peripheral nerves , has been revealed to cause a change of connections among central neurons [1,2,3]. As a common type of PNP, postherpetic neuralgia (PHN) is caused by the reactivation of the varicella zoster virus, which travels along nerve cells, and produces pain in the infected region [4]. In fact, PHN is a prototypical human chronic neuropathic condition for exhibiting multiple signs of peripheral and central neuropathy [5]. Some studies have explored the effects of PHN pain on brain activity [6,7,8]. Their results showed that brain activations with spontaneous PHN pain included affective, sensory-discriminative, emotion, hedonics, reward, and punishment areas. And most of activations decreased after treatment by Lidoderm [7]. Also the connectivity between several regions and putamen was altered for PHN patients [8]. Up to now, however, there is no investigation concerning topological organization of functional networks in the whole brain related to PHN pain. The small-world networks is an attractive model to describe complex networks by providing quantitative parameters [9,10], given that functional connectivity between different brain regions was modulated by PHN [8], the small-world brain functional networks are hypothesized in the current study with their properties altered by PHN pain.

**Materials and Methods:** Twenty-six right-handed subjects (13 patients suffering from PNH and 13 control healthy subjects) participated in the study (7 males, 6 females for both groups). The average age of the PHN group was 65.9 (range 52-77) and that of the healthy controls was 64.5 (range 52-76) years old (two tailed t-test, p = 0.78). PHN pain was localized on the left side of body region for the 13 patients. All of these patients were assessed using a mechanical Visual Analog Scale (VAS), with a range from 0 (no pain) to 10 (the highest tolerable pain) to rate the pain intensity levels [7,8]. The thirteen patients were with pain intensities ranged from 6.5 to 9 on VAS (average score: about 7.6 points). The duration of persistent pain was longer than two months for all patients. During the time of scanning, the greatest care was taken to avoid the situation that might trigger evoked pain. During the MR scanning, all subjects were instructed to keep their eyes closed, minds clear, and awakening remained. The scan time was 8.5 minutes for all subjects.

All MRI experiments were performed using a General Electric 3T Signa system (GE Medical Systems, Waukesha, WI) with a standard head coil. Functional data were acquired using a double readout spiral-out sequence with simultaneous Gradient-echo blood oxygenation level dependent (BOLD) and cerebral blood flow (CBF) acquisitions, at short and long TEs, respectively [11,12]. Both readouts utilized slice thickness / gap (THK) of 8.0 / 2.0 mm with 3.6 x 3.6 $mm^2$ in-plane resolution, using a 230 $mm^2$ field of view (FOV) with a 64 x 64 acquisition matrix, a repetition time (TR) of 3000 ms and a 90° flip angle. CBF/BOLD readouts were acquired at TEs of 3.1/30 ms, respectively, covering 12 axial slices of the whole cerebrum. The set consisted of 170 functional contiguous axial images.

Only the BOLD data were analyzed in this study. After discarding the first 10 images, the remained 160 functional images were first corrected for the acquisition time delay among different slices and motion corrected, then coregistered with the corresponding anatomical image to facilitate transformation to Montreal Neurological Institute (MNI) space and resampling of functional images to isotropic 2*2*2 $mm^3$ voxels. The data were detrended and temporally filtered by band-pass (0.01~0.08 Hz).The data sets preprocessed above were divided into 90 regions of interest (ROIs) (45 for each hemisphere) according to the AAL-atlas [13]. The mean time series of each region were then obtained by averaging the time series of all voxels in that area. Several sources of spurious variances (six motion parameters, the signal averaged from the region in cerebrospinal fluid, and the signal averaged from the region in the white matter) were further removed by multiple linear regression analysis. The Pearson correlation coefficients between every possible pair of the regional residual time series were calculated, and a 90*90 correlation matrices were obtained for each subject. Then a Fisher's r-to-z transformation was applied to the correlation matrices to improve the normality of the correlation coefficients, and the z-score matrices were obtained. Finally, each absolute z-score matrix was thresholded into an undirected binary graph (network) for further analysis by graph theoretical approaches with the nodes describing brain regions and the edges describing the links between the regions.

In the study, the network cost (0.05 to 0.4, with an incremental interval of 10 edges) was used for threshold measurement [9,14]. Several small-world parameters of the networks were obtained, including clustering coefficient ($C_p$), characteristic path length ($L_p$), global efficiency ($E_{glob}$), local efficiency ($E_{loc}$), integrated regional nodal efficiency (i.e. the area under the curve with the cost ranged from 0.05 to 0.4 for regional nodal efficiency). [9,15,16]. To estimate the small-world properties, 100 degree-matched random networks were generated.

**Results:** At a wide range of cost threshold, the brain networks of the PHN group demonstrated lower clustering coefficients and local efficiencies compared with the healthy controls. Statistical analysis further revealed that there were significantly differences (two-sample two-tailed t-test ,$P < 0.05$) in $C_p$ values ($0.09 < \text{cost} < 0.1525$, black asterisks in Fig1) and local efficiencies ($0.1025 < \text{cost} < 0.1075$, 0.1125, $0.1175 < \text{cost} < 0.23$,black asterisks in Fig1) in a range of cost, whereas there was no significant difference in $L_P$ and $E_{glob}$ between the two groups. To further reveal the influence on regionally nodal characteristics of the brain networks, the group differences in integrated nodal efficiency were compared (two-sample two-tailed t-test, $P < 0.05$). The PHN case demonstrated significant decreases of nodal efficiency in the right inferior orbitofrontal cortex, pallidum, left paraHippocampal gyrus, fusiform gyrus，thalamus and inferior temporal gyrus and increases in the left olfactory cortex in comparison with the healthy controls. These results suggest that the nodal efficiency of brain functional networks was profoundly affected by PHN.

**Discussion and Conclusion:** Although both the PHN and healthy controls showed small-world attributes in their brain functional networks (higher $C_p/E_{loc}$ and an approximately equivalent $L_p/E_{glob}$ in comparison with random networks) [9,10], the decreased $C_P$ and $E_{loc}$ combined with non-significantly changed $L_P$ and $E_{glob}$ for PHN compared with healthy subjects made the network topology of PHN exhibit tendency of a shift toward random networks (see Fig 1). In summary, this is the first study to reveal small-world properties of brain functional networks in PHN. A tendency of shift toward random networks for PHN was observed. Moreover, the nodal efficiency was altered for PHN. Our results suggested that the widely distributed functional brain networks were altered in PHN, thus providing further evidence for brain dysfunction associated with PHN.

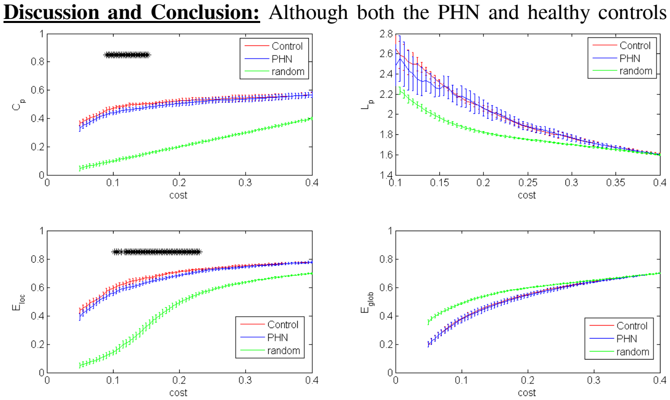


Fig 1 The $C_p$, $L_p$ , $E_{loc}$ and $E_{glob}$ for the random, PHN and healthy controls brain networks as a function of the cost (the cost for $L_p$ was ranged from 0.1 to 0.5, which can prevent infinit value for disconnected networks).

**Reference:** [1] Price DD, Science 2000;288:1769-1772.[2] Cauda F et al., Plos One 2009 ;4:e4542.[3] Vartiainen N et al., J Pain 2009;10(8):854-859.[4] Cadogan MP, J Gerontol Nurs 2001;36:10-14.[5] Oaklander AL, Pain 2001;92:139-145.[6] Iadarola MJ et al., Pain 1995; 63:55-64.[7]Geha PY et al., Pain 2007;128:88-100.[8]Geha PY et al., Pain 2008;138 : 641–656.[9] Achard S et al., PLoS Comput Biol 2007;3: e17.[10] Watts DJ et al., Nature 1998;393:440–442.[11] Wong EC et al., NMR Biomed 1997;10: 237-249.[12] Wong EC et al., Magn Reson Med 1998;39:702-708.[13] Tzourio-Mazoyer N et al., Neuroimage 2002;15:273–289.[14] Latora V et al., Phys Rev Lett 2001;87:198701.[15] He Y et al., Brain 2009; 32: 3366–3379.[16] Liu B et al., Plos One 2012;7: e39342.